

# Efficiency Evaluation of Different TiO<sub>2</sub> Coatings on the Photocatalytic Inactivation of Airborne Bacterial Spores

Silvia M. Zacarías,<sup>†</sup> María L. Satuf,<sup>†</sup> María C. Vaccari,<sup>‡</sup> and Orlando M. Alfano<sup>\*,†</sup>

<sup>†</sup>Instituto de Desarrollo Tecnológico para la Industria Química (Universidad Nacional del Litoral and Consejo Nacional de Investigaciones Científicas y Técnicas), Ruta Nacional No. 168, 3000 Santa Fe, Argentina

<sup>‡</sup>Facultad de Bioquímica y Ciencias Biológicas, Universidad Nacional del Litoral, Ruta Nacional No. 168 Paraje el Pozo, 3000 Santa Fe, Argentina

**ABSTRACT:** The performance of different TiO<sub>2</sub> coatings is compared for the photocatalytic inactivation of dry *Bacillus subtilis* spores dispersed on TiO<sub>2</sub> films under UV-A radiation. Three different TiO<sub>2</sub> coatings were assayed: Degussa P-25, sol-gel, and composite sol-gel/Degussa P-25. The influence of the increase in the number of TiO<sub>2</sub> layers was also studied. Furthermore, the amount of TiO<sub>2</sub> deposited on the borosilicate glass plates and the fraction of energy effectively absorbed by the catalytic films were determined. Spectral diffuse transmittance and reflectance measurements were performed using a spectroradiometer with an integrating-sphere attachment. The net-radiation method was then applied to evaluate the fraction of energy absorbed by the coatings. To objectively compare the performance of the catalytic films, two types of efficiencies were calculated: the photonic efficiency and the quantum efficiency of inactivation. The highest quantum efficiency was obtained with the TiO<sub>2</sub> Degussa P-25 coating with two layers.

## 1. INTRODUCTION

Indoor air pollution represents a major risk to human health. Indoor air pollutants include chemical compounds, particulate matter, and biological contaminants present in the form of bioaerosols. The latter consist of bacterial cells and cellular fragments, bacterial and fungal spores, and byproducts of microbial metabolism, which can be present as particulates, liquids, or volatile organic compounds.<sup>1</sup>

Under unfavorable conditions, vegetative cells of bacilli are able to undergo a differentiation process called sporulation. This process is a survival mechanism in the face of nutrient deprivation. Bacterial spores have no metabolism and can withstand a wide range of environmental assaults, including heat, desiccation, UV light, and the action of deleterious chemicals.<sup>2</sup> Also, dormant spores can be found in virtually every type of environment on Earth.<sup>3</sup> Despite such extreme dormancy, spores maintain an alert sensory mechanism that enables them to respond to specific nutrients. This leads to germination and outgrowth to form a new vegetative cell.<sup>4</sup>

Heterogeneous photocatalysis, an advanced oxidation technology that uses UV-A radiation (300–400 nm) coupled with a TiO<sub>2</sub> catalyst, is a potential alternative to mitigate the problem of biological contamination in the indoor environment. When TiO<sub>2</sub> is photoexcited by UV-A light, it is well-known that the formation of electron–hole pairs occurs with the generation of oxidative radical species and that these radical species can cause fatal damage against microorganisms in contact with the catalytic surface. The process does not involve any expensive oxidizing chemicals and can be performed under ambient conditions of temperature and pressure.

The pioneering work in the field of gas-phase photocatalytic disinfection was done by Goswami et al.,<sup>5</sup> who reported the total inactivation of *Serratia marcescens* in a photocatalytic reactor with recirculation using Degussa P-25 TiO<sub>2</sub>. Afterward,

several studies on the application of photocatalysis to inactivate bacteria<sup>6–10</sup> and spore-forming bacteria<sup>11–17</sup> over TiO<sub>2</sub>-coated surfaces were published.

Despite the numerous scientific articles devoted to the mechanisms and modeling of photocatalysis for disinfection purposes, recently compiled in several review papers,<sup>18–20</sup> only a few studies have focused on evaluating the performance of catalytic systems by means of efficiency parameters.<sup>21–23</sup> The accurate evaluation of the inactivation activity of different supports is essential for selecting the best photocatalyst and improving the design of disinfection systems. Efficiency parameters relate the inactivation rate of microorganisms to the energy reaching the photocatalyst (photonic efficiency) or absorbed by the photocatalyst (quantum efficiency), thus allowing a comparison of results obtained under different experimental conditions. Using a different approach, Faure et al.<sup>24</sup> studied the inactivation of *E. coli* by different TiO<sub>2</sub> supports and calculated the proportion of photons effectively absorbed by the photocatalyst by means of a Monte Carlo simulation. Then, they plotted the bacterial concentration as a function of the quantity of photons absorbed and compared different supports for an equivalent UV-A dose.

In a previous work, the inactivation of *B. subtilis* spores over TiO<sub>2</sub> thin films obtained with a sol-gel technique was studied and modeled, but the time required to inactivate the microorganisms was relatively long.<sup>25</sup> In the present study, to improve the photocatalytic inactivation efficiency, three different coatings were assayed: Degussa P-25 TiO<sub>2</sub>, sol-gel TiO<sub>2</sub>, and sol-gel/Degussa P-25 TiO<sub>2</sub>. The amount of TiO<sub>2</sub>

**Received:** April 16, 2012

**Revised:** September 21, 2012

**Accepted:** September 24, 2012

**Published:** September 24, 2012

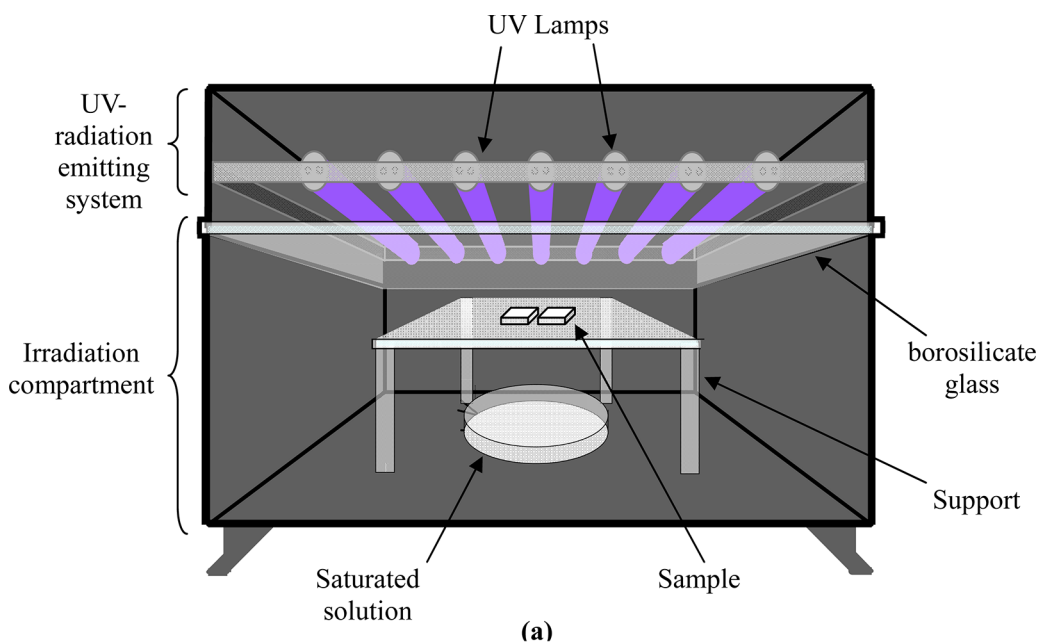


**Figure 1.** Experimental setup: (a) schematic diagram, (b) top view.

deposited on the borosilicate glass plates and the fraction of energy effectively absorbed by the catalytic films were also determined. Measurements of the spectral diffuse transmittance and reflectance of bare and  $\text{TiO}_2$ -coated borosilicate glass plates were obtained with a spectroradiometer equipped with an integrating-sphere reflectance attachment. Afterward, the net-radiation method was used to compute the fraction of energy absorbed by the  $\text{TiO}_2$  films as a function of wavelength. Finally, to objectively compare the performance of the three different coatings, the photonic efficiency and the quantum efficiency of inactivation were calculated and compared.

## 2. MATERIALS AND METHODS

**2.1. Experimental Setup.** The photocatalytic experiments were carried out in an experimental setup consisting of a UV-radiation emitting system, an irradiation compartment, and a support to hold the coated glass plates with the spore samples during irradiation (Figure 1). A borosilicate glass separated the UV emitting system from the irradiation compartment. The UV-radiation emitting system consisted of a set of seven tubular black-light fluorescent lamps (YLX 8W/BLB) held by a metallic rectangular box above the irradiation compartment in a horizontal parallel arrangement. The emission of the lamps was between 300 and 400 nm, with a maximum at about 350

nm (UV-A). Figure 2 shows the spectral emission of the lamps, as well as the diffuse transmittance and reflectance of the

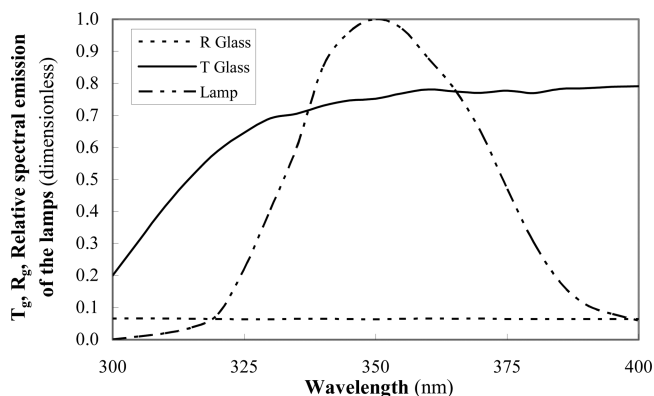


**Figure 2.** Relative spectral emission of the lamps (---) and diffuse transmittance (—) and reflectance (- - -) of the borosilicate glass.

borosilicate glass. More details about the experimental setup can be found elsewhere.<sup>25</sup>

Inside the irradiation compartment, local measurements of the radiation flux incident at different positions on a plane were made using a radiometer (ILT 1700, International Light Technologies). Only the most illuminated surface, placed at the central zone of the irradiation compartment, was employed for the experiments. The average incident net radiation flux obtained was  $1.89 \text{ mW cm}^{-2}$ , which is equivalent to  $2.01 \times 10^{-5} \text{ Einstein cm}^{-2} \text{ h}^{-1}$  (or  $1.21 \times 10^{19} \text{ photon cm}^{-2} \text{ h}^{-1}$ ). Conversion from energy content ( $\text{mW cm}^{-2}$ ) to photon content ( $\text{Einstein cm}^{-2} \text{ h}^{-1}$ ) was made with Planck's equation, considering the total emission spectrum of the lamps (shown in Figure 2). It should be noted that the measurement of the incident radiation flux was performed by placing the radiometer below the borosilicate glass that separated the lamps from the irradiation compartment; therefore, the value obtained takes into account the absorption of the aforementioned borosilicate glass.

Photocatalytic plates with spore samples were held horizontally in the central zone of the irradiation compartment, where the radiation flux was almost uniform. A saturated solution of ammonium sulfate was included in the irradiation compartment to secure an atmosphere with a high and constant relative humidity, necessary to obtain sustainable  $\text{TiO}_2$  photocatalytic activity. Throughout the experiments, the relative humidity and temperature inside the irradiation compartment were kept constant at 70% and  $40^\circ\text{C}$ , respectively. A thermohygrometer (Oakton Thermohygrometer Kit) was employed to measure these variables.

**2.2. Photocatalyst Preparation.** The photocatalytic inactivation of *Bacillus subtilis* spores was assayed over three different  $\text{TiO}_2$  coatings. The first one (Degussa P-25  $\text{TiO}_2$ ) used a suspension of  $150 \text{ g L}^{-1}$  of Degussa P-25  $\text{TiO}_2$  (Evonik Degussa) in ultrapure water (Osmonion Ultrapure Water, Apema) at a pH value of 1.5 (adjusted with  $\text{HNO}_3$ ). The required amount of photocatalyst was dispersed in ultrapure water at the indicated pH and then sonicated for 2 h.<sup>26</sup>

The second coating (sol-gel  $\text{TiO}_2$ ) was obtained by a sol-gel method using titanium tetraisopropoxide as the precursor.<sup>27</sup> First, the hydrolysis of titanium tetraisopropoxide was conducted in an acid aqueous medium. Ultrapure water was mixed with concentrated nitric acid (Anedra, 65%), and

titanium isopropoxide (Sigma Aldrich, 97%) was added to this mixture. Under such conditions, the hydrolysis of the precursor proceeded vigorously, producing large lumps of hydrated  $\text{TiO}_2$ . The dispersion of the lumped particles was achieved by stirring the suspension over a period of 10 h at  $80^\circ\text{C}$ , until a clear sol of  $\text{TiO}_2$  nanoparticles was obtained.

The third coating (sol-gel/Degussa P-25  $\text{TiO}_2$ ) was obtained by a composite sol-gel/Degussa P-25  $\text{TiO}_2$  technique.<sup>28</sup> Denatured ethanol (85% ethanol + 15% methanol) was mixed with high-purity ultrapure water and concentrated HCl (36.5%). Alcohol was used as the solvent to prevent fast hydrolysis of titanium alkoxide. HCl was employed in this process to control the rate of condensation and avoid fast gelation of the sol. After a few minutes of agitation, titanium tetraisopropoxide (Sigma Aldrich, 97%) was added to the mixture. Hydrolysis was carried out by dropwise addition of the precursor to the prepared solution, under stirring. This mixture was agitated for 2 h. After this period, Degussa P-25  $\text{TiO}_2$  was added, and the mixture was stirred for 12 h.

**2.3. Preparation of Photocatalytic Plates.** Before  $\text{TiO}_2$  immobilization, the borosilicate glass plates were washed with a solution containing 20 g of potassium hydroxide, 250 mL of isopropyl alcohol, and 250 mL of ultrapure water. The plates remained in contact with the washing solution for 24 h and then for 2 h under sonication (Ultrasonik 300). Afterward, they were heated for 8 h at  $500^\circ\text{C}$  to remove any trace of organic material that might still remain on the surface. The size of the plates was always  $2 \text{ cm} \times 2 \text{ cm}$ .

For the three coatings tested, the  $\text{TiO}_2$  immobilization on the glass plates was achieved by the dip-coating technique, with a withdrawal speed of  $3 \text{ cm min}^{-1}$  at room temperature ( $25^\circ\text{C}$ ). However, after being applied, the three photocatalysts were treated differently. For the coatings with Degussa P-25  $\text{TiO}_2$ , the plates were dried in an oven at  $110^\circ\text{C}$  for 24 h and then heated at  $500^\circ\text{C}$  for 2 h at a heating rate of  $5^\circ\text{C min}^{-1}$ . For the sol-gel  $\text{TiO}_2$  coating, the plates were dried in an oven at  $80^\circ\text{C}$  for 1 h and then heated at  $200^\circ\text{C}$  for 6 h. Finally, for the sol-gel/Degussa P-25  $\text{TiO}_2$  coating, the plates were dried at room temperature ( $25^\circ\text{C}$ ) for 1 h and then heated at  $500^\circ\text{C}$  for 2 h at a heating rate of  $11^\circ\text{C min}^{-1}$ .

When it was necessary to apply two or three layers of photocatalyst to the glass plates, after the drying and heating steps, the next coating layer was applied by repeating the procedure used to deposit the first layer. In particular, it was not possible to apply a third layer with the sol-gel/Degussa P-25  $\text{TiO}_2$  technique because of the poor adhesive properties of the obtained film.

**2.4. Characterization of Photocatalytic Plates.**  
**2.4.1. Calculation of Absorbed Radiation.** The superficial rate of photon absorption by the catalytic films,  $e_f^{a,s}$ , averaged over the irradiated area  $A_{\text{irr}}$  can be expressed as<sup>23</sup>

$$\langle e_f^{a,s} \rangle_{A_{\text{irr}}} = \langle q_{f,\text{in}} \rangle_{A_{\text{irr}}} - \langle q_{f,\text{tr}} \rangle_{A_{\text{irr}}} - \langle q_{f,\text{rf}} \rangle_{A_{\text{irr}}} = \langle q_{f,\text{in}} \rangle_{A_{\text{irr}}} \alpha_f \quad (1)$$

where  $q_{f,\text{in}}$  is the local radiative flux that reaches the coated plate,  $q_{f,\text{tr}}$  is the local radiative flux transmitted through the catalytic plate,  $q_{f,\text{rf}}$  is the local radiative flux reflected by the  $\text{TiO}_2$  surface, and  $\alpha_f$  is the fraction of energy absorbed by the  $\text{TiO}_2$  film. From eq 1,  $\alpha_f$  can be calculated as

$$\alpha_f = \frac{\langle q_{f,\text{in}} \rangle_{A_{\text{irr}}} - \langle q_{f,\text{tr}} \rangle_{A_{\text{irr}}} - \langle q_{f,\text{rf}} \rangle_{A_{\text{irr}}}}{\langle q_{f,\text{in}} \rangle_{A_{\text{irr}}}} \quad (2)$$

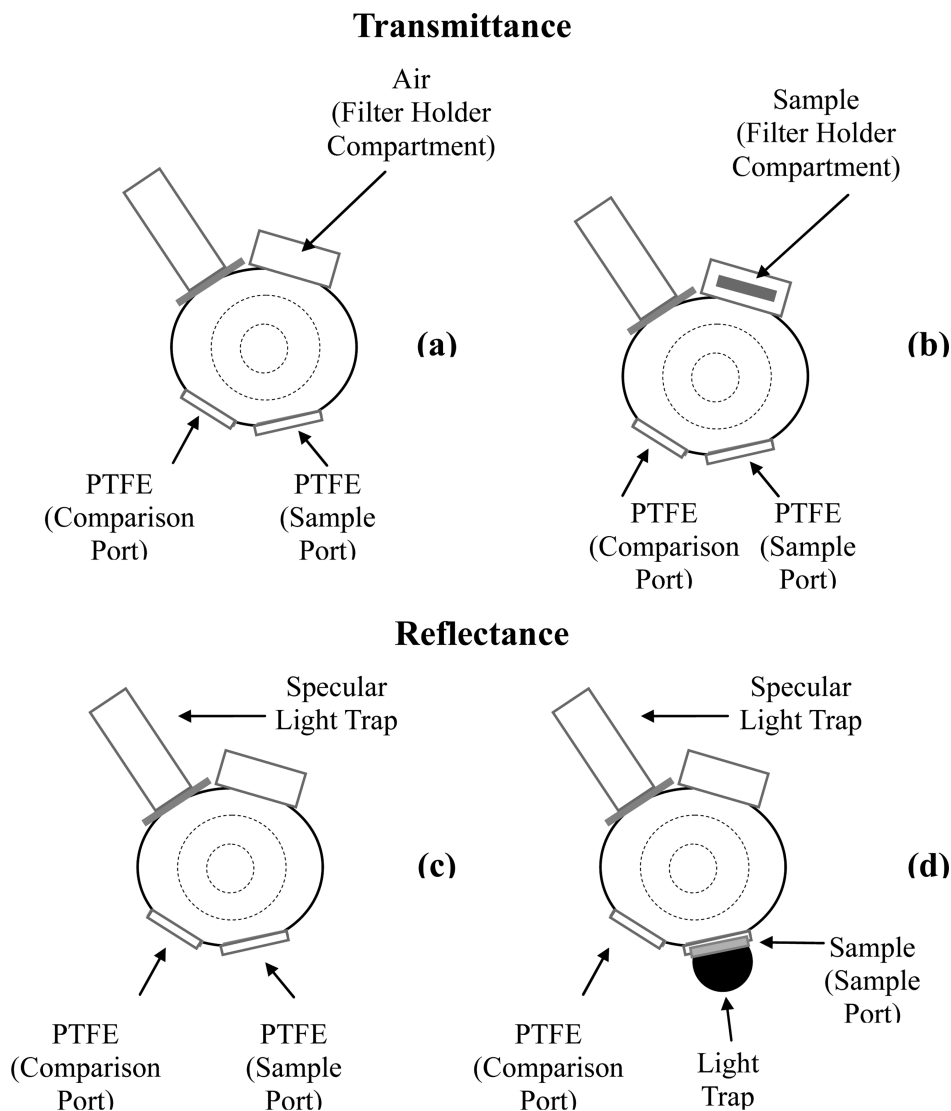


**Figure 3.** Integrating-sphere configurations: (a,b) transmittance measurements, (c,d) reflectance measurements.

To compute  $\alpha_p$ , the net-radiation method was employed.<sup>29</sup> This method considers energy absorption, reflection, and transmission produced by multiple parallel layers. The final mathematical expressions used to calculate the fractions of incident energy transmitted ( $T$ ), reflected ( $R$ ), and absorbed ( $\alpha$ ) are given by

$$T_{fg} = \frac{T_f T_g}{1 - R_f R_g} \quad (3)$$

$$R_{fg} = R_f + \frac{R_g T_f^2}{1 - R_f R_g} \quad (4)$$

$$\alpha_f = 1 - T_f - R_f \quad (5)$$

where  $f$ ,  $g$ , and  $fg$  represent film, glass, and film + glass, respectively. The values of  $T_{fg}$  and  $R_{fg}$  were obtained by spectrophotometric measurements of diffuse transmittance and reflectance, respectively, of the coated plates. It should be noted that these quantities depend on the wavelength of the incident radiation.

**2.4.2. Transmittance and Reflectance Measurements.** Diffuse reflectance and transmittance measurements of the

coated plates were made on an Optronic OL series 750 spectroradiometer equipped with an OL 740-70 integrating-sphere reflectance attachment. The device consists of a source attachment (deuterium and tungsten lamps), a monochromator, and an integrating sphere. The integrating sphere is composed of a system of mirrors that routes the beam of light to the necessary position. Also, it has two openings in the wall for reflecting samples, namely, the sample port and the comparison port, and a filter holder compartment for transmittance measurements. The detector is situated in the central part of the integrating sphere (Figure 3).

The methodology employed to record reflectance and transmittance spectra is similar to that described in Satuf et al.<sup>30</sup> for obtaining the optical properties of  $\text{TiO}_2$  suspensions. However, in the present work, this methodology was modified to measure uncoated and  $\text{TiO}_2$ -coated borosilicate glass plates. Readings were made in the UV region, with wavelengths ranging from 300 to 400 nm. The integrating-sphere configurations for measurements are schematically shown in Figure 3a–d. For diffuse transmittance measurements, two pressed poly(tetrafluoroethylene) (PTFE) reflectance standards were placed in the comparison and sample ports of the sphere. A transmittance reading of 100% was obtained against

air (Figure 3a). To measure the transmittance of the sample, the glass coated with the photocatalyst was placed in the filter holder compartment (Figure 3b). For diffuse reflectance measurements, a PTFE reflectance standard was used as the reference in the comparison port. A reflectance reading of 100% was obtained by placing another PTFE standard in the sample port (Figure 3c). To measure the reflectance of the sample, the glass with the TiO<sub>2</sub> was placed in the sample port with its back covered by a light trap that absorbed all transmitted radiation, with the PTFE standard still in the comparison port (Figure 3d).

**2.4.3. Determination of the Amount of Photocatalyst Immobilized over Glass Plates.** The amount of TiO<sub>2</sub> deposited on the borosilicate glass plates was measured by a spectrophotometric procedure adapted from Jackson et al.<sup>31</sup> that involves the digestion of the photocatalyst followed by a colorimetric detection. The solution used to dissolve the TiO<sub>2</sub> (solution A) was prepared by mixing 10 g of (NH<sub>4</sub>)<sub>2</sub>SO<sub>4</sub> into 25 mL of concentrated H<sub>2</sub>SO<sub>4</sub>. Each coated glass was placed in a receptacle containing 4 mL of solution A. The mixture of TiO<sub>2</sub>-coated glass in solution A was boiled until the TiO<sub>2</sub> was completely dissolved (about 1 h) and cooled, and then, 6 mL of ultrapure water were added. All of the liquid was quantitatively transferred to a 25-mL volumetric flask. The flask was filled to exactly 25 mL with a 5/95 volume percent solution of concentrated H<sub>2</sub>SO<sub>4</sub>/H<sub>2</sub>O. Three drops of H<sub>2</sub>O<sub>2</sub> were added to 10 mL of the solution and then stirred. Finally, the absorbance of the colored solution was measured at 410 nm (Perkin-Elmer Lambda 35 UV/vis spectrophotometer). A calibration curve was constructed by adding different weighed amounts of Degussa P-25 TiO<sub>2</sub> to solution A and then following the same procedure as described for the plates.

**2.5. Spore Formation and Collection.** The model microorganism used in this work was *Bacillus subtilis* (ATCC 6633 strain). Following the technique proposed by Shehata and Collins,<sup>32</sup> suspensions of spores in distilled water were prepared. To do this, a Roux bottle containing a sporulation medium, consisting of nutritive agar (Merck Chemicals) with 0.05% MnSO<sub>4</sub> and 0.05% MgSO<sub>4</sub>, was inoculated and incubated at 30 °C for a 7–10-day period. Then, the spores and vegetative cells obtained were recovered by washing the surface of the sporulation medium with sterile buffer phosphate (pH 6.8). After this step, the spores recovered were centrifuged three times for 15 min each at 3500 rpm with the same buffer. The suspension was kept at 30 °C for 48–72 h to induce vegetative cell lysis. Then, the vegetative cells and the spores were washed again according to the instructions outlined above. This procedure was repeated three times to wash the cells. The spores were finally suspended in sterile distilled water and conserved at 4 °C.

**2.6. Irradiation of Spore Samples and Measurement of Spore Viability.** To ensure the absence of vegetative cells before carrying out the irradiation experiments, the spore suspension was held for 10 min at 80 °C. Next, 10 μL of this suspension was uniformly spread over the surface of each coated glass plate (2.25 cm<sup>2</sup>) and dried at 50 °C for 30 min. Afterward, these plates were placed in the irradiation compartment and exposed to UV-A radiation for different time periods (2, 4, 6, or 8 h). The remaining viable spores were counted according to the technique detailed elsewhere.<sup>25</sup> The tests were repeated twice for each experimental condition studied, and the counting of the viable spores of each repetition was made in duplicate.

The decay of viable spores as a function of the irradiation time was fitted with the exponential equation

$$N = N_0 e^{-kt} \quad (6)$$

where  $N$  (CFU cm<sup>-2</sup>) is the bacterial concentration,  $N_0$  (CFU cm<sup>-2</sup>) is the initial bacterial concentration,  $k$  (h<sup>-1</sup>) is the kinetic constant, and  $t$  (h) is the time.

**2.7. Photocatalytic Efficiency Calculation.** Two types of photocatalytic inactivation efficiencies were evaluated: the photonic efficiency  $\eta_{\text{app}}$ , also known as the apparent quantum efficiency, and the quantum efficiency of inactivation  $\eta_{\text{abs}}$ .

$\eta_{\text{app}}$  is defined as the ratio of the initial photocatalytic inactivation rate to the rate of radiation energy reaching the plate covered with the TiO<sub>2</sub> film, over the entire range of wavelengths under consideration

$$\eta_{\text{app}} = \frac{-(dN/dt)|_{t=0}}{\langle q_{f,\text{in}} \rangle_{A_{\text{irr}}}} \quad (7)$$

where  $\langle q_{f,\text{in}} \rangle_{A_{\text{irr}}}$  is the area-average radiative flux that reaches the coated plate. The value of  $\langle q_{f,\text{in}} \rangle_{A_{\text{irr}}}$  experimentally obtained using a radiometer (section 2.1), was  $1.21 \times 10^{19}$  photon cm<sup>-2</sup> h<sup>-1</sup>.

On the other hand,  $\eta_{\text{abs}}$  can be defined as the ratio of the initial photocatalytic inactivation rate to the rate of the absorbed radiation energy within the useful wavelength range

$$\eta_{\text{abs}} = \frac{-(dN/dt)|_{t=0}}{\langle e_f^{a,s} \rangle_{A_{\text{irr}}}} = \frac{-(dN/dt)|_{t=0}}{\langle q_{f,\text{in}} \rangle_{A_{\text{irr}}} \sum_{\lambda} \alpha_{f,\lambda} \phi_{\lambda}} \quad (8)$$

where  $\phi_{\lambda}$  is a normalized distribution function of the wavelengths that reach the coated plates.  $\phi_{\lambda}$  takes into account the spectral emission of the lamps and the slight modification of the lamp spectrum produced by the absorption of the borosilicate glass that separates the lamps from the irradiation compartment, mainly at wavelengths lower than 340 nm (see Figure 2).

### 3. RESULTS

#### 3.1. Characterization of the Photocatalytic Plates.

**3.1.1. Spectrophotometric Determination of the Photocatalyst Quantity over the Plates.** The quantity of TiO<sub>2</sub> deposited on the borosilicate glass plates, measured by the spectrophotometric determination adapted from Jackson et al.,<sup>31</sup> is reported in Table 1, where each determination was done in triplicate. As expected, a gradual increase in the TiO<sub>2</sub> content (mg cm<sup>-2</sup>) with the number of coating layers was observed.

**Table 1. Amount of TiO<sub>2</sub> (mg cm<sup>-2</sup>) Deposited on the Glass Plates**

coating	one layer	two layers	three layers
Degussa P-25 TiO <sub>2</sub>	1.26	1.77	2.13
sol-gel TiO <sub>2</sub>	0.05	0.11	0.16
sol-gel/Degussa TiO <sub>2</sub>	0.58	2.01	–

**3.1.2. Optical Characterization.** Figure 4 presents the diffuse transmittance and reflectance spectra of the borosilicate glass coated with Degussa P-25 TiO<sub>2</sub>, sol-gel TiO<sub>2</sub>, and sol-gel/Degussa TiO<sub>2</sub>, for the corresponding number of layers assayed. For each coating technique, different optical behaviors were observed, in direct relation to the amount of TiO<sub>2</sub> deposited on each sample. The Degussa and Degussa/sol-gel

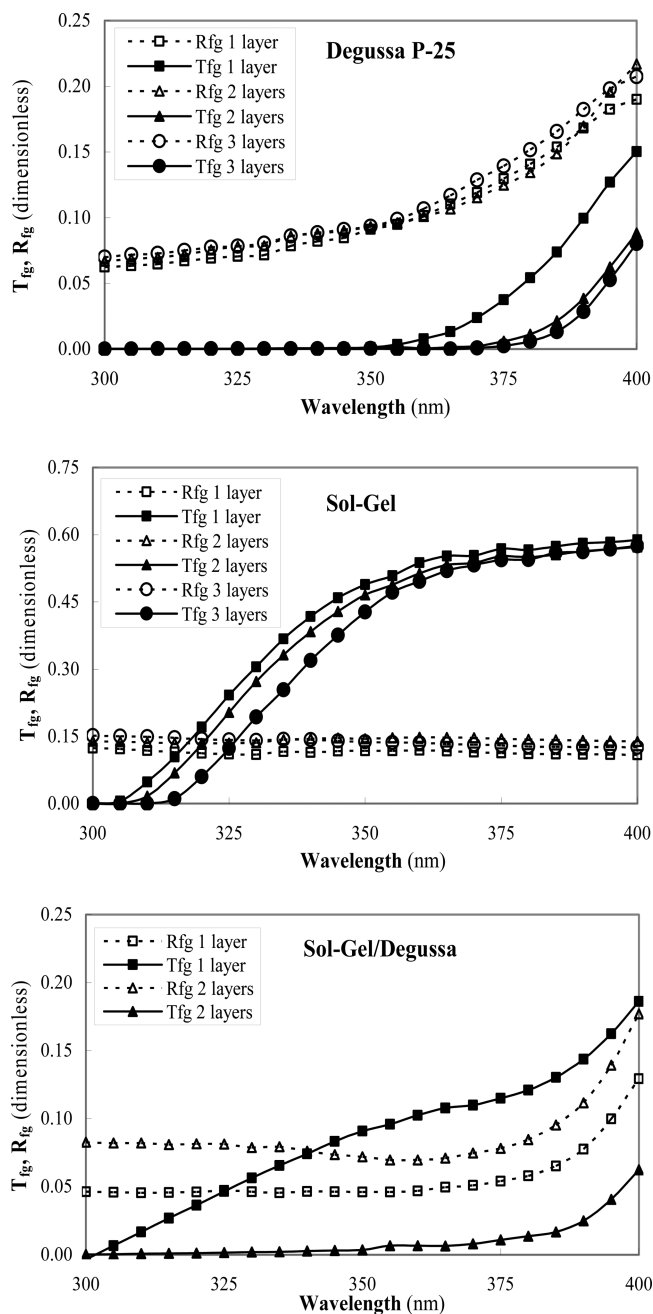


**Figure 4.** Experimental transmittance ( $T_{fg}$ ) and reflectance ( $R_{fg}$ ) values.

coatings presented significantly greater absorptions than the sol-gel samples, especially at wavelengths lower than 375 nm. Nevertheless, a gradual increase in the absorption of radiation with the number of layers was noticed for the three types of coatings. These experimental results, along with other characteristics of the films, are analyzed in section 4.

**Table 2.** Calculated Values of  $T_f$ ,  $R_f$ , and  $\alpha_f$  for a Wavelength of 350 nm

	Degussa P-25 TiO <sub>2</sub>			sol-gel TiO <sub>2</sub>			sol-gel/Degussa TiO <sub>2</sub>	
	one layer	two layers	three layers	one layer	two layers	three layers	one layer	two layers
$T_f$	0.002	<0.001	<0.001	0.646	0.615	0.565	0.121	0.005
$R_f$	0.091	0.093	0.094	0.091	0.120	0.120	0.045	0.072
$\alpha_f$	0.907	0.907	0.906	0.263	0.265	0.318	0.834	0.923

Using eqs 3 and 4 and the experimental values of transmittance and reflectance presented in Figures 2 and 4, we evaluated  $T_f$  and  $R_f$  and then calculate  $\alpha_f$  (eq 5) between 300 and 400 nm. Table 2 shows an example of the results obtained at the most important wavelength (350 nm). The absorbed fraction ( $\alpha_f$ ) was relatively high for the coatings made with Degussa P-25 TiO<sub>2</sub> and sol-gel/Degussa TiO<sub>2</sub>, whereas for the sol-gel TiO<sub>2</sub> coating, this fraction was considerably lower.

To complete the characterization of the plates, SEM images of coating surfaces were obtained. Figure 5 shows the images

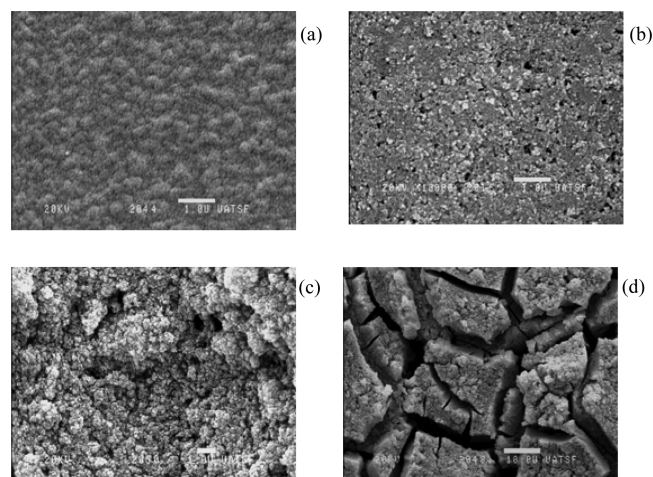


**Figure 5.** SEM images of the TiO<sub>2</sub> coating surfaces with two layers: (a) sol-gel, (b) Degussa P-25, (c,d) sol-gel/Degussa. The white bar represents (a-c) 1 and (d) 10  $\mu\text{m}$ .

corresponding to the three coatings assayed with two layers. The coating obtained with the sol-gel method (Figure 5a) presents the most uniform surface. The Degussa P-25 image (Figure 5b) reveals a more irregular surface, where dark regions of uncoated glass are observed. The roughest surface was obtained with the composite technique (Figure 5c,d), with considerable irregularities throughout the plate. This unevenness is better observed in Figure 5d, at lower magnification. It should be noted that the adherence of the composite coating to the glass was also poor.

Additionally, the film thickness for the coating with the highest quantum efficiency of all tested samples, the Degussa P-25 coating with two layers, was estimated from SEM images of the cross section of the TiO<sub>2</sub> plates (images not shown). The approximate value measured was 14  $\mu\text{m}$ .

**3.2. Spore Inactivation Results.** Figure 6 shows the experimental results and the curve fittings using eq 6 obtained in the photocatalytic inactivation of *Bacillus subtilis* spores over the plates coated with Degussa, sol-gel, and sol-gel/Degussa TiO<sub>2</sub>. Error bars represent the 99% confidence intervals. It is worth noting that no detectable changes in the survival of

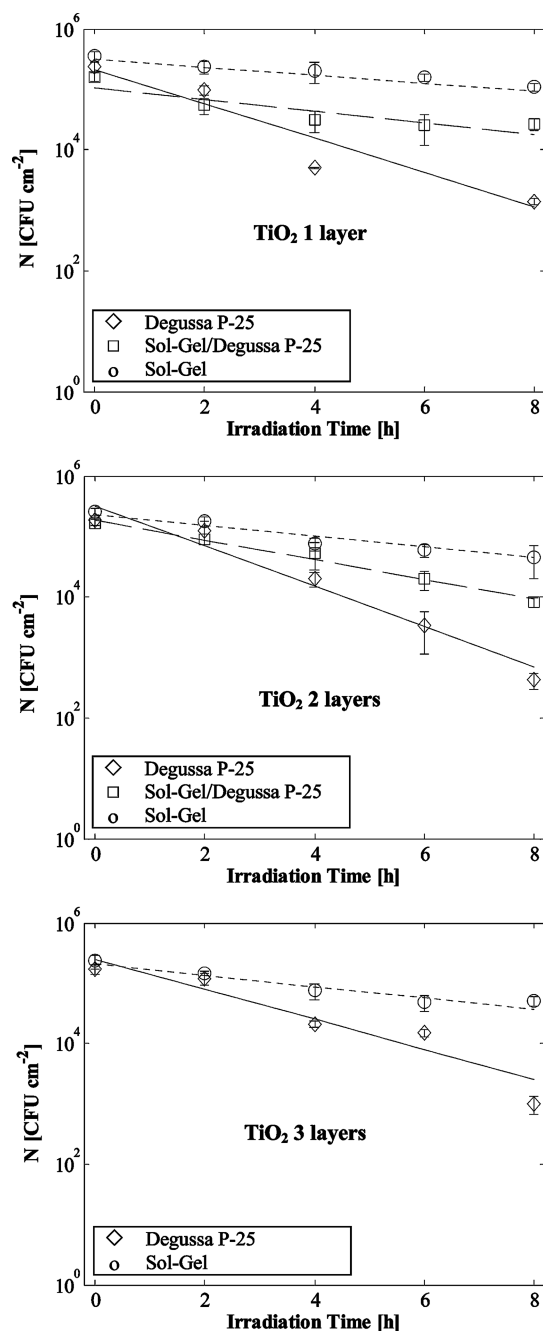


**Figure 6.** Spore inactivation curves for the three coating techniques. Experimental values: ( $\diamond$ ) Degussa P-25  $\text{TiO}_2$ , ( $\square$ ) sol-gel/Degussa P-25  $\text{TiO}_2$ , ( $\circ$ ) sol-gel  $\text{TiO}_2$ . Fittings (—, - - -, - - -).

spores were observed when the samples were kept in the dark or in the absence of photocatalyst.

It can be noticed that, when *B. subtilis* spores were irradiated over  $\text{TiO}_2$  surfaces, their viability decreased significantly, and

the extent of inactivation increased with the irradiation time. Values of the parameters in eq 6, namely,  $N_0$  and  $k$ , for each coating and each number of layers are reported in Table 3.

**3.3. Evaluation of Photocatalytic Efficiencies.** To compute the photonic and quantum efficiencies, the initial photocatalytic inactivation rates are needed (numerators of eqs 7 and 8). These values were calculated from the slope of the inactivation curves (Figure 6) and are listed in Table 4. Also, the values of the energy absorbed by the coated plates (denominator of eq 8) are presented in the table. The denominator of eq 7 (incident radiation flux) was always  $1.21 \times 10^{19}$  photon  $\text{cm}^{-2}$   $\text{h}^{-1}$ .

The final results for both photocatalytic efficiencies are summarized in Table 5 for each photocatalyst studied and for the different layers tested. It should be noted that  $\eta_{\text{abs}}$  more closely represents the efficiency of the photocatalytic inactivation of the bacterial spores because it considers not only the radiation reaching the plate but the rate of energy effectively absorbed by the catalytic film.

#### 4. DISCUSSION

For the Degussa coating, a high percentage of the incident radiation was absorbed by the three samples tested, as evidenced by the values of  $\alpha_f$  in Table 2 and  $\langle e_f^{3,5} \rangle_{\text{Air}}$  in Table 4. Moreover, an appreciable increment in the amount of immobilized  $\text{TiO}_2$  was found as the number of layers increased. It is noted that the highest inactivation rate was obtained with two layers. Because the amount of absorbed energy was similar for the three samples, the quantum efficiency was also higher for the plate with two layers of  $\text{TiO}_2$ . In fact, the highest quantum efficiency of all tested samples was obtained with the Degussa coating with two layers:  $\eta_{\text{abs}} = 2.27 \times 10^{-14}$  (Table 5). Between one and two layers, an appreciable increment in the amount of immobilized  $\text{TiO}_2$  was found (Table 1). Therefore, it was expected that a greater inactivation of spores would be obtained because of the increase in the amount of photocatalyst available to interact with the microorganisms. With three layers, although the amount of photocatalyst was higher than that with two layers, the inactivation rate was lower and similar to that found with one layer. A possible explanation can be found in the surface roughness of the obtained film with three layers. Bacterial spores could lie in the irregularities of the coating where radiation could not impinge.<sup>33</sup> In addition, an excessive production of hydroxyl radicals could lead to the formation of hydroperoxyl radicals, which are less effective for bacteria inactivation.<sup>34</sup> At high  $\text{TiO}_2$  concentrations, as is the case for three layers, the reactions represented by eqs 9 and 10 could contribute to the diminution of bacterial inactivation. In eq 9,  $\bullet\text{OH}$  dimerizes to form  $\text{H}_2\text{O}_2$ , which, in turn, produces  $\text{HO}_2\bullet$  (eq 10). The hydroperoxyl radical is less reactive than the hydroxyl radical and does not contribute significantly to the oxidative process.



**Table 3.** Estimated Parameters of Eq 6

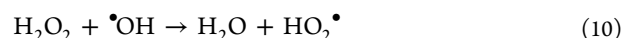
coating	$N_0$ (CFU $\text{cm}^{-2}$ )			$k$ ( $\text{h}^{-1}$ )		
	one layer	two layers	three layers	one layer	two layers	three layers
Degussa P-25 $\text{TiO}_2$	$2.13 \times 10^5$	$3.20 \times 10^5$	$2.48 \times 10^5$	0.655	0.767	0.572
sol-gel $\text{TiO}_2$	$2.87 \times 10^5$	$2.31 \times 10^5$	$2.18 \times 10^5$	0.139	0.202	0.225
sol-gel/Degussa $\text{TiO}_2$	$1.06 \times 10^5$	$1.85 \times 10^5$	—	0.221	0.375	—

Table 4. Initial Inactivation Rates and Energy Absorbed by Each Coating

coating	$-(dN/dt)_{t=0}$ (CFU cm <sup>-2</sup> h <sup>-1</sup> )			$\langle e_{\text{eff}}^{\text{ph}} \rangle_{\text{arr}}$ (photon cm <sup>-2</sup> h <sup>-1</sup> )		
	one layer	two layers	three layers	one layer	two layers	three layers
Degussa P-25 TiO <sub>2</sub>	$1.40 \times 10^5$	$2.45 \times 10^5$	$1.42 \times 10^5$	$1.07 \times 10^{19}$	$1.08 \times 10^{19}$	$1.08 \times 10^{19}$
sol-gel TiO <sub>2</sub>	$3.99 \times 10^4$	$4.67 \times 10^4$	$4.91 \times 10^4$	$3.36 \times 10^{18}$	$3.39 \times 10^{18}$	$4.01 \times 10^{18}$
sol-gel/Degussa TiO <sub>2</sub>	$2.34 \times 10^4$	$6.94 \times 10^4$	–	$1.00 \times 10^{19}$	$1.11 \times 10^{19}$	–

Table 5. Photocatalytic Inactivation Efficiencies (CFU photon<sup>-1</sup>)

coating	$\eta_{\text{app}}$ ( $\times 10^{14}$ )			$\eta_{\text{abs}}$ ( $\times 10^{14}$ )		
	one layer	two layers	three layers	one layer	two layers	three layers
Degussa P-25 TiO <sub>2</sub>	1.15	2.02	1.17	1.31	2.27	1.32
sol-gel TiO <sub>2</sub>	0.33	0.39	0.40	1.19	1.37	1.22
sol-gel/Degussa TiO <sub>2</sub>	0.19	0.57	–	0.23	0.63	–



Also, an increase in the recombination rate of electrons and holes produced by the excess of catalytic particles could contribute to the decrease of the inactivation rate.<sup>33</sup> Our results are in accordance with those obtained by van Grieken et al.<sup>26</sup> in wall and fixed-bed reactors employed for the inactivation of *E. coli* aqueous suspensions. Immobilization of TiO<sub>2</sub> was performed by the same procedure as used in the present work, the maximum activity was found with two layers of coating, and a clear decrease in the inactivation rate was obtained when the reactors were coated with three layers of photocatalyst.

For the coatings obtained by the sol-gel technique, a gradual increase in the TiO<sub>2</sub> content with the number of layers was found, resulting in increases in the absorption of radiation, inactivation rate, and photonic efficiency. However, regarding  $\eta_{\text{abs}}$ , the sample with two layers was the most efficient; in this case, it can be noted from Table 4 that the increase of the energy absorbed by the coating with three layers (denominator of eq 8) was higher than the slight increase of the initial inactivation rate (numerator of eq 8). It is worth highlighting that the amount of photocatalyst and the percentage of radiation absorbed were significantly lower than those obtained with the Degussa coating, although the values of the quantum efficiency of inactivation were similar.

Finally, a significant increment in the amount of immobilized TiO<sub>2</sub> was found with the sol-gel/Degussa coating between one and two layers. Increases in the radiation absorption, inactivation rate, and efficiency parameters with the number of layers were also obtained. The maximum absorption of all tested samples was achieved with two layers of the composite catalyst (92%). Regarding the transmittance and reflectance spectra, we can affirm that the remaining 8% of radiation was lost by reflection (the transmittance of this sample was almost null). Although the coatings obtained with the sol-gel/Degussa technique contained high amounts of TiO<sub>2</sub> and absorbed high percentages of the incident radiation, the inactivation rates were similar to those obtained with the sol-gel samples, and the values of  $\eta_{\text{abs}}$  were the lowest among the three coating techniques. This behavior can be ascribed to the undesired increase in the recombination of electron/hole pairs and hydroxyl radicals, as discussed previously in the case of the Degussa coating with three layers. A deficiency in the contact of

the spores with the surface of the composite coatings can also explain the relatively low inactivation rate values.<sup>24</sup> This possibility is supported by the SEM images, which revealed significant irregularities in the composite coating surface (Figure 5c,d).

The efficiency values obtained in this work can be compared with those recently reported by Briggiler Marcó et al.<sup>23</sup> They studied the photocatalytic inactivation efficiency of 10 bacteriophages dispersed on TiO<sub>2</sub>-coated plates exposed to UV-A radiation for different periods of time and found the highest inactivation efficiency for the bacteriophage J-1 ( $2.273 \times 10^{-12}$  PFU photon<sup>-1</sup>). This efficiency value is 2 orders of magnitude higher than that found in our work for Degussa P-25 TiO<sub>2</sub> coating with two layers (Table 5). This variation might be due to the structural differences between the J-1 bacteriophage and the *B. subtilis* spore. In general, virus structures are much simpler than those corresponding to bacterial spores.

Also, Marugán et al.<sup>22</sup> studied the photocatalytic disinfection of *E. coli* in aqueous suspensions. They also found photonic efficiency values higher than those obtained in this work, on the order of  $10^{-11}$  CFU photon<sup>-1</sup>. In this case, the model microorganism was a vegetative bacterium, which is much less complex than a bacterial spore.

## 5. CONCLUSIONS

The highest efficiency of all tested samples was obtained with the Degussa P-25 TiO<sub>2</sub> coating with two layers. This result can be attributed to the characteristics of the film, which (i) contained a high amount of TiO<sub>2</sub>, rendering high absorption of the incident radiation, and (ii) presented a regular surface, which enhanced the contact between the spores and the photocatalytic particles.

The calculation of efficiency parameters represents a valuable tool for comparing different catalytic systems. The photonic efficiency  $\eta_{\text{app}}$  and the quantum efficiency of inactivation  $\eta_{\text{abs}}$  can be used to evaluate the performance of coatings. Nevertheless,  $\eta_{\text{abs}}$  provides more useful information because it shows how efficiently the absorbed radiation is employed to inactivate microorganisms, providing an indirect insight into the photocatalytic mechanism. Also, it can guide the design of better coatings, as the results can provide evidence for deficient contact between bacteria and photocatalyst or poor absorption of radiation.

## AUTHOR INFORMATION

### Corresponding Author

\*Tel.: +54-342-4511546. Fax: +54-342-4511170. E-mail: alfano@santafe-conicet.gov.ar.

### Notes

The authors declare no competing financial interest.

## ACKNOWLEDGMENTS

The authors are grateful to Universidad Nacional del Litoral (UNL), Consejo Nacional de Investigaciones Científicas y



Técnicas (CONICET), and Agencia Nacional de Promoción Científica y Tecnológica (ANPCyT) for financial support. We also thank Antonio C. Negro for his valuable help during the experimental work and Professor Maria C. Lurá for her valuable support.

## NOMENCLATURE

- $A_{\text{irr}}$  = irradiated area ( $\text{cm}^2$ )  
 $e_{\text{p}}^{\text{ps}}$  = superficial rate of photon absorption by the  $\text{TiO}_2$  catalytic films (photon  $\text{cm}^{-2} \text{h}^{-1}$ )  
 $k$  = kinetic constant ( $\text{h}^{-1}$ )  
 $N$  = viable spore concentration (CFU  $\text{cm}^{-2}$ )  
 $N_0$  = initial viable spore concentration (CFU  $\text{cm}^{-2}$ )  
 $q_{\text{fin}}$  = local radiative flux that reaches the  $\text{TiO}_2$  catalytic films (photon  $\text{cm}^{-2} \text{h}^{-1}$ )  
 $q_{\text{fr}}$  = local radiative flux reflected by the  $\text{TiO}_2$  catalytic films (photon  $\text{cm}^{-2} \text{h}^{-1}$ )  
 $q_{\text{tr}}$  = local radiative flux transmitted through the  $\text{TiO}_2$  catalytic films (photon  $\text{cm}^{-2} \text{h}^{-1}$ )  
 $R$  = reflectance  
 $t$  = time (h)  
 $T$  = transmittance

## Acronyms

- ATCC = American Type Culture Collection  
 CFU = colony forming units  
 PTFE = poly(tetrafluoroethylene)

## Greek Letters

- $\alpha_f$  = fraction of energy absorbed by the  $\text{TiO}_2$  films  
 $\eta$  = photocatalytic inactivation efficiency (CFU photon $^{-1}$ )  
 $\phi_\lambda$  = distribution function of the wavelengths that reach the  $\text{TiO}_2$  catalytic films

## Subscripts

- abs = denotes the quantum efficiency of inactivation  
 app = denotes the photonic efficiency (or apparent quantum efficiency)  
 f = relative to a property of the  $\text{TiO}_2$  film  
 fg = relative to a property of the  $\text{TiO}_2$  film + glass  
 g = relative to a property of the bare borosilicate glass plate  
 $\lambda$  = relative to a specific wavelength

## Special Symbol

- $\langle \rangle$  = average

## REFERENCES

- Stetzenbach, L. D.; Buttner, M. P.; Cruz, P. Detection and enumeration of airborne biocontaminants. *Curr. Opin. Biotechnol.* **2004**, *15*, 170.
- Atrih, A.; Foster, S. J. The role of peptidoglycan structure and structural dynamics during endospore dormancy and germination. *Antonie van Leeuwenhoek* **1999**, *75*, 299.
- Moeller, R.; Horneck, G.; Facius, R.; Stackebrandt, E. Role of pigmentation in protecting *Bacillus* sp. endospores against environmental UV radiation. *FEMS Microbiol. Ecol.* **2005**, *51*, 231.
- Atrih, A.; Foster, S. J. Bacterial endospores the ultimate survivors. *Int. Dairy J.* **2002**, *12*, 217.
- Goswami, D. Y.; Trivedi, D. M.; Block, S. S. Photocatalytic disinfection of indoor air. *J. Sol. Energ. Eng.* **1997**, *119*, 92.
- Goswami, T. K.; Hingorani, S. K.; Greist, H. Photocatalytic System to Destroy Bioaerosols in Air. *J. Adv. Oxid. Technol.* **1999**, *4*, 185.
- Josset, S.; Taranto, J.; Keller, N.; Keller, V.; Lett, M. C.; Ledoux, M. J.; Bonnet, V.; Rougeau, S. UV-A photocatalytic treatment of high flow rate air contaminated with *Legionella pneumophila*. *Catal. Today* **2007**, *129*, 215.
- Pal, A.; Pehkonen, S. O.; Yu, L. E.; Ray, M. B. Photocatalytic Inactivation of Airborne Bacteria in a Continuous-Flow Reactor. *Ind. Eng. Chem. Res.* **2008**, *47*, 7580.
- Paschoalino, M. P.; Jardim, W. F. Indoor air disinfection using a polyester supported  $\text{TiO}_2$  photoreactor. *Indoor Air* **2008**, *18*, 473.
- Josset, S.; Keller, N.; Lett, M.-C.; Ledoux, M. J.; Keller, V. Numeration methods for targeting photoactive materials in the UV-A photocatalytic removal of microorganisms. *Chem. Soc. Rev.* **2008**, *37*, 744.
- Wolfrum, E. J.; Huang, J.; Blake, D. M.; Maness, P.; Huang, Z.; Fiest, J. Photocatalytic oxidation of bacteria, bacterial and fungal spores, and model biofilm components to carbon dioxide on titanium dioxide coated surfaces. *Environ. Sci. Technol.* **2002**, *36*, 3412.
- Lin, C. Y.; Li, C. S. Inactivation of microorganisms on the photocatalytic surfaces in air. *Aerosol Sci. Technol.* **2003**, *37*, 939.
- Pal, A.; Min, X.; Yu, L. E.; Pehkonen, S. O.; Ray, M. Photocatalytic inactivation of bioaerosols by  $\text{TiO}_2$  coated membrane. *Int. J. Chem. React. Eng.* **2005**, *3*, A45.
- Vohra, A.; Goswami, D. Y.; Deshpande, D. A.; Block, S. S. Enhanced photocatalytic inactivation of bacterial spores on surfaces in air. *J. Ind. Microbiol. Biotechnol.* **2005**, *32*, 364.
- Zhao, J.; Krishna, V.; Hua, B.; Moudgil, B.; Koopman, B. Effect of UV-A irradiance on photocatalytic and UV-A inactivation of *Bacillus cereus* spores. *J. Photochem. Photobiol. B.* **2009**, *94*, 96.
- Chuaybamroong, P.; Chotigawin, R.; Supothina, S.; Sribenjalux, P.; Larpiattaworn, S.; Wu, C.-Y. Efficacy of photocatalytic HEPA filter on microorganism removal. *Indoor Air* **2010**, *20*, 246.
- Prasad, G. K.; Ramacharyulu, P. V. R. K.; Merwyn, S.; Agarwal, G. S.; Srivastava, A. R.; Singh, B.; Rai, G. P.; Vijayaraghavan, R. Photocatalytic inactivation of spores of *Bacillus anthracis* using titania nanomaterials. *J. Hazard. Mater.* **2011**, *185*, 977.
- Dalrymple, O. K.; Stefanakos, E.; Trotz, M. A.; Goswami, D. Y. A review of the mechanisms and modeling of photocatalytic disinfection. *Appl. Catal. B* **2010**, *98*, 27.
- Chong, M. N.; Jin, B.; Chow, C. W. K.; Saint, C. Recent developments in photocatalytic water treatment technology: A review. *Water Res.* **2010**, *44*, 2997.
- Foster, H. A.; Ditta, I. B.; Varghese, S.; Steele, A. Photocatalytic disinfection using titanium dioxide: Spectrum and mechanism of antimicrobial activity. *Appl. Microbiol. Biotechnol.* **2011**, *90*, 1847.
- de Lasa, H.; Serrano, B.; Salaces, M. *Photocatalytic Reaction Engineering*; Springer Publishing: New York, 2005.
- Marugán, J.; van Grieken, R.; Sordo, C.; Cruz, C. Kinetics of the photocatalytic disinfection of *Escherichia coli* suspensions. *Appl. Catal. B* **2008**, *82*, 27.
- Briggiler Marcó, M.; Quiberoni, A. L.; Negro, A. C.; Reinheimer, J. A.; Alfano, O. M. Evaluation of the photocatalytic inactivation efficiency of dairy bacteriophages. *Chem. Eng. J.* **2011**, *172*, 987.
- Faure, M.; Gerardin, F.; André, J.-C.; Ponsa, M.-N.; Zahraa, O. Study of photocatalytic damages induced on *E. coli* by different photocatalytic supports (various types and  $\text{TiO}_2$  configurations). *J. Photochem. Photobiol. A* **2011**, *222*, 323.
- Zacarias, S. M.; Vaccari, M. C.; Irazoqui, H. A.; Imoberdorf, G. E.; Alfano, O. M. Effect of the radiation flux on the photocatalytic inactivation of spores of *Bacillus subtilis*. *J. Photochem. Photobiol. A* **2010**, *214*, 171.
- van Grieken, R.; Marugán, J.; Sordo, C.; Pablos, C. Comparison of the photocatalytic disinfection of *E. coli* suspensions in slurry, wall and fixed-bed reactors. *Catal. Today* **2009**, *144*, 48.
- Yamazaki-Nishida, S.; Nagano, K. J.; Phillips, L. A.; Cervera-March, S.; Anderson, M. A. Photocatalytic degradation of trichloroethylene in the gas phase using  $\text{TiO}_2$  pellets. *J. Photochem. Photobiol. A* **1993**, *70*, 95.
- Keshmiri, M.; Mohseni, M.; Troczynski, T. Development of novel  $\text{TiO}_2$  sol-gel-derived composite and its photocatalytic activities for trichloroethylene oxidation. *Appl. Catal. B* **2004**, *53*, 209.
- Siegel, R.; Howell, J. *Thermal Radiation Heat Transfer*, 4th ed.; Taylor and Francis: New York, 2002.

(30) Satuf, M. L.; Brandi, R. J.; Cassano, A. E.; Alfano, O. M. Experimental Method to Evaluate the Optical Properties of Aqueous Titanium Dioxide Suspensions. *Ind. Eng. Chem. Res.* **2005**, *44*, 6643.

(31) Jackson, N. B.; Wang, C. M.; Luo, Z.; Schwitzgebel, J.; Ekerdt, J. G.; Brock, J. R.; Heller, A. Attachment of TiO<sub>2</sub> Powders to Hollow Glass Microbeads: Activity of the TiO<sub>2</sub>-Coated Beads in the Photoassisted Oxidation of Ethanol to Acetaldehyde. *J. Electrochem. Soc.* **1991**, *138*, 3660.

(32) Shehata, T. E.; Collins, E. B. Sporulation and heat resistance of psychrophilic strains of *Bacillus*. *J. Dairy Sci.* **1972**, *55*, 1405.

(33) Caballero, L.; Whitehead, K. A.; Allen, N. S.; Verran, J. Inactivation of *Escherichia coli* on immobilized TiO<sub>2</sub> using fluorescent light. *J. Photochem. Photobiol. A* **2009**, *202*, 92.

(34) Rincon, A. G.; Pulgarin, C. Photocatalytical inactivation of *E. coli*: Effect of (continuous–intermittent) light intensity and of (suspended–fixed) TiO<sub>2</sub> concentration. *Appl. Catal. B* **2003**, *44*, 263.